International Immunopharmacology 83 (2020) 106460

Contents lists available at ScienceDirect

International Immunopharmacology

journal homepage: www.elsevier.com/locate/intimp

Assessment of oral ciprofloxacin impaired gut barrier integrity on gut bacteria in mice

Shengyun Zhu[a,b,c], Huiqi Li[a,b], Jing Liang[a,b], Chaoran Lv[a,b], Kai Zhao[a,b,c], Mingshan Niu[a,b,c], Zhenyu Li[a,b,c], Lingyu Zeng[a,b,c], Kailin Xu[a,b,c,*]

[a] Institute of Blood Diseases, Xuzhou Medical University, Xuzhou, Jiangsu Province 221002, China
[b] Department of Hematology, Affiliated Hospital of Xuzhou Medical University, Xuzhou, Jiangsu Province 221002, China
[c] Key Laboratory of Bone Marrow Stem Cell, Xuzhou, Jiangsu Province 221002, China

ARTICLE INFO

Keywords:
Ciprofloxacin
Indole
Short chain fat acids
Gut bacteria
Epithelial cells
IL-17A

ABSTRACT

Gut bacteria and gut barrier plays important roles in body homeostasis. Ciprofloxacin (CPFX) is widely used to treat bacterial infections. However, whether high dosage of CPFX has side effects on gut barrier integrity is still unclear. Our results indicated that the High CPFX treatment (1 mg/ml) caused weight loss, nervousness, anorexia, and increased apoptosis cells in gut, but less influence was observed in the Low CPFX group (0.2 mg/ml). Meanwhile, the High CPFX treatment impaired tight junction molecules *Ocln/ZO-1* level and down-regulated antibacterial genes expression (*reg3γ, pla2g2α and defb1*). Further, the High CPFX treatment increased pro-inflammatory cytokine IL-1β in intestinal tract, decreased *IL-17A* of duodenum but increased *IL-17A* of colon at day 37. In addition, the gut bacterial diversity and richness behaved significantly loss regarding CPFX treatment, especially in the High CPFX group during the experiment. Indole exhibited sharply decline in both Low and High CPFX groups at day 7, and the High CPFX mice needed longer time on restoring indole level. Meanwhile, CPFX treatment strongly decreased the concentrations of butyric acid and valeric acid at day 1. Correlation analysis indicated that the linked patterns between the key bacteria (families *Bacteroidales_S247*, *Ruminococcaceae* and *Desulfovibrionaceae)* and metabolites (indole and butyric acid) were disturbed via the CPFX treatment. In conclusion, the High CPFX treatment impaired the gut barrier with the evidence of reduced expression of tight junction proteins, increased apoptosis cells and inflammatory cells, decreased the bacterial diversity and composition, which suggesting a proper antibiotic-dosage use should be carefully considered in disease treatment.

1. Introduction

Trillions of microorganisms reside in the human gastrointestinal tract, and the connection between host and gut bacteria is mutually beneficial for host health, because of its influence on metabolism, energy balance, inflammation and more [1]. Complex interactions of gut bacteria, epithelium and gut-associated lymphoid tissue are involved in regulating immunity responses [2]. Previous studies point out that the human commensal *Bacteroides fragilis* is able to deliver immunomodulatory molecules to immune cells via secreting outer membrane vesicles [3]; *segmented filamentous bacteria* and *Helicobacter* are identified as the dominated taxa during T cell responses to gut bacteria and these consortia are closely adherent to the epithelium [4]. *Lachnospiracea* showed a negative correlation with IL-17A [5]. Probiotic strain *Lactobacillus acidophilus* has been shown to modulate feces microbiota and its associated metabolic phenotype in aging mice [6]. Therefore, maintaining the mutual interactions between host and gut bacteria are orchestrated to achieve body homeostasis.

Major functions of gut bacteria are concerned in metabolic activities which absorb nutrients and energy, thus impacts on intestinal epithelia and immune responses for pathogens invasion. Indole, derived from L-tryptophan digested by symbiotic bacteria in gut, plays a key role in cytoplasm signaling pathway and gut homeostasis regulation [7–9]. Previous studies suggested that oral indole containing capsules can enhance the expression of patients' tight junction proteins and decrease the risk of colitis [8]. Moreover, prior study confirmed that indole replaced glucose as energy supply can improve barrier functions of intestinal epithelial cells (IECs) [10]. Furthermore, short chain fatty acids (SCFAs) such as butyric acid, is a favored energy source for IECs and may work as an important factor linking the tight junctions of IECs via activation of AMP-activated protein kinase [11].

Ciprofloxacin (CPFX), a fluoroquinolone class, is widely used to

* Corresponding author at: No. 99 Huaihai West Road, Department of Hematology, Affiliated Hospital of Xuzhou Medical University, Xuzhou, 221002, China.
E-mail address: lihmd@163.com (K. Xu).

https://doi.org/10.1016/j.intimp.2020.106460
Received 18 November 2019; Received in revised form 13 March 2020; Accepted 28 March 2020
1567-5769/ © 2020 Elsevier B.V. All rights reserved.

treat or prevent certain bacterial infections such as urinary tract infections, pneumonia, and gastrointestinal infections [12]. Increasing CPFX consumption leads to selection of resistant mutants among nosocomial pathogens and these resistant strains can more easily spread than strains resistant to other drugs [13]. Reduced susceptibility to CPFX has become a major problem mostly in Asia [14]. Previous studies have shown that exposure to antibiotics can predispose individuals to conditions adverse side effects, such as gut microbiota dysbiosis, inflammatory bowel disease [15]. In this study, different dosages of CPFX were administrated to C57BL/6 mice to investigate their relationships and figured out the high dosage of CPFX impaired gut barrier integrity and altered the linked patterns between some bacteria and indole/butyrate. Here, we highlighted the effects of CPFX on gut IECs and bacteria so as to improve the proper use of antibiotic. Alteration by CPFX of this crosstalk is sufficient to induce a state of dysbiosis and the injury of intestinal tract.

2. Materials and methods

2.1. Animal treatment

C57BL/6 mice, male, ages 5–6 weeks and weighing 20 g to 21 g, were purchased from Beijing Vital River Laboratory Animal Technology Co., Ltd., China. The mice were housed in sterilized cages (five mice per cage) in a special pathogen free room at the Experimental Animal Center of Xuzhou Medical University for 1 week prior to experiments. Three groups of mice (n = 10) were treated with autoclaved water alone (Control), 1 mg/ml CPFX (High CPFX, for gastrointestinal decontamination [16]) or 0.2 mg/ml CPFX (Low CPFX) in drinking water for 2 weeks and refreshed every day, then allowed to recover from antibiotic exposure until day 37. Feces from each group were collected regularly throughout all experiments. We changed fresh radiated-corn cob padding one night before feces collection and collections were processed in the next morning. All samples were immediately flash-frozen in liquid nitrogen and stored at −80 °C until use. Daily clinical mice parameters (diarrhoea, weight, anorexia or nervousness etc.) were recorded twice a week. All animal care and experimental procedures followed ethical standards of animal use and were approved by Xuzhou Medical University.

2.2. TUNEL apoptosis assay

Duodenum and colon were fixed in 4% paraformaldehyde at day 14 and were embedded in paraffin blocks, cut to 4 μm sections. The TUNEL apoptosis assay was performed according to the experimental procedure (KeyGEN BioTECH, Nanjing, China). Green, apoptosis cells; Blue, nuclear.

2.3. ELISA assay

The concentrations of LPS in serum and MPO in intestinal tissue homogenization were detected using mouse ELISA kits (RenjieBio, Shanghai, China) according to the experimental procedure.

2.4. Western blotting (WB)

Duodenum, jejunum, ileum, and colon were lysed with radio immunoprecipitation assay buffer (1 mM phenylmethylsulfonyl fluoride) and by automatic sample rapid grinding machine (Jingxin, Shanghai, China), and supernatants were collected after spinning [17]. Proteins were separated in 12% sodium dodecyl sulfate-polyacrylamidegel electrophoresis gels, transferred to nitrocellulose filter membrane (GeneralElectric Company, Buckinghamshire, United Kingdom) and immunoblotted overnight at 4 °C with appropriate primary antibodies specific for IL-1β, β-actin (Santa Cruz Biotechnology, Santa Cruz, CA), and Ocln (Proteintech group, Hubei, China). After incubating with secondary antibodies, the membranes were washed with PBS (1% Tween 20), then films were developed with an enhanced chemi-luminescence kit (Bio-Rad, Hercules, CA).

2.5. DNA extraction and 16S rRNA gene amplicon sequencing

The total DNA was extracted from 0.1 g to 0.2 g feces by the FastDNA Spin kit for soil (MP Biomedical, USA) followed the manufacturer's protocol. DNA quality was tested by 1% sodium boric acid agarose gel electrophoresis, and DNA concentrations were measured by NanoDrop 1000 spectrophotometer (Thermo Scientific, Waltham, MA, USA). The bacterial and archaeal 16S rRNA gene was amplified by the 338F (5'-ACTCCTACGGGAGGCAGCAG-3') and 806R (5'-GGACTACHVGGGTWTCTAAT-3') primer pair [18–20] modified with adapters and barcodes using TransGen AP221-02:TransStart Fastpfu DNA Polymerase. The purified PCR products were loaded for sequencing on the MiSeq Illumina platform (Majorbio Bio-Pharm Technology Co., Ltd., Shanghai, China).

The 16S profile analysis is done by QIIME (Quantitiative Insights Into Microbial Ecology) pipelines, the raw DNA sequence was firstly filtered to remove low quality reads (quality < 20 and ambiguity codes) and sequence length shorter than 50 bp. Then the high quality sequences were clustered into operational taxonomic unit (OTU) at 97% sequence identity level via the UPARSE imbedded in QIIME and selected the most abundant sequence to representative sequence for each OTU. Taxonomic classification of the sequences with different levels was simultaneously classified by the RDP and Silva database with the online version [21,22]. The high-quality sequences were get and used for microbial diversity analyses and visualization. The alpha diversity including rarefaction curves, Shannon diversity index, species richness and other calculation were done used by QIIME and R platform for each sample. Raw sequences were submitted to the National Center for Biotechnology Information and sequence data were deposited at the Sequence Read Archive under the accession number SRP134025.

2.6. Indole detection

After feces were collected into microtubes, a 10-fold volume of methanol was added and incubated at 4 °C for 4 h. The mixture was homogenized by sonication and centrifuged at 20,000 g for 15 min at 4 °C, and then the supernatant was filtered with 0.22 μm membrane. We collected the filtered supernatant applied to HPLC analysis (Agilent 1200 Series HPLC-DAD-FLD system, Agilent Technologies, USA). Indoles were monitored by UV detection at 280 nm coupled with Zorbax Eclipse XDB-C8 (150 × 4.60 nm, 3.5 um) column. The mobile phase consisted of (A) 0.01% formic acid in water and (B) acetonitrile; the flow rate was set at 1 mL/min and the injection volume was 20 μL. The contents of indole compounds in different samples, for which standards were available, were calculated from the calibration curves generated by the integration of areas of absorption peaks determined during analysis.

2.7. SCFAs measurement

Mice feces were homogenized in distilled water for SCFAs measurement (acetic acid, propionic acid, butyric acid, and valeric acid) and then filtrated via 0.22 μm membrane filter before injection. A high performance liquid chromatography (Agilent1260 Infinity Quaternary, California, USA) equipped with a SPD-20A UV/Vis detector monitored at 215 nm for VFAs. The VFAs were simultaneously analyzed through a HPX-87H column (300 × 7.8 mm) (Bio-Rad, Hercules, CA) and kept at 55 °C, flow 0.5 mL/min, eluent 0.045 N H_2SO_4 with 6% acetonitrile (v/v) [23].

Table 1
Primer sequences of real-time PCR.

primer	Forward sequence (5′-3′)	Reverse sequence (5′-3′)	NCBI#	Product size (bp)
β-actin	ATGGAGGGGAATACAGCCC	TTCTTTGCAGCTCCTTCGTT	NM_007393.5	149
Muc2	ATGCCCACCTCCTCAAAGAC	GTAGTTTCCGTTGGAACAGTGAA	NM_023566.4	101
Reg3γ	AGCCACAAGCAAGATCCCAA	GGCCATAGTGCACACAGAGT	NM_011260.2	138
Pla2g2α	AAGGATCCCCCAAGGATGCCAC	CAGCCGTTTCTGACAGGAGTTCTGG	NM_001082531.1	167
Defb1	AACACGGTACACAGGCTTCC	GGATGCGCTCTGGTTGGACA	NM_007843.3	140
Ocln	CCTACTCCTCCAATGGCAAA	CTCCCCACCTGTCGTGTAGT	NM_008756.2	254
ZO-1	GCAGACTTCTGGAGGTTTCG	CTTGCCAACTTTTCTCTGGC	NM_001163574.1	194
IL-17A	ATCCACCTCACACGAGGCACAA	AGATGAAGCTCTCCCTGGACTCAT	NM_010552.3	81

2.8. Real-time quantitative PCR

The tissues were lysed with Trizol (Invitrogen, Thermo Fisher, Shanghai, China) by automatic sample rapid grinding machine following previous methods [24]. Total RNA was reverse transcribed using the Transcriptor first strand cDNA synthesis kit (Roche, Basel, Switzerland) and analyzed on Roche Light Cycler 480 with light cycler 480 SYBR Green I master. All data were normalized to the expression of *β-actin*. The primer sequences were as Table 1.

2.9. Statistical analysis

Datasets are presented as mean ± SEM. At least 3 independent experiments were performed for each assay. For comparison between Control and different dosages of CPFX, data were assessed by 1-way ANOVA using GraphPad Prism software. A P value < 0.05 indicates statistically significance. Statistical significant was marked as different P levels ($^{*}p < 0.05$, $^{**}p < 0.01$, $^{***}p < 0.001$, $^{****}p < 0.0001$). The statistical calculations of microbial dataset were based on R (version 3.4.2) software packages with vegan, gplots and corrplot.

3. Results

3.1. CPFX induced weight loss and apoptosis cells in gut depending on different dosages in mice

The effects of different CPFX levels on gut integrity were studied as shown in Fig. 1a. High CPFX (1 mg/ml) and Low CPFX (0.2 mg/ml) added in autoclaved drinking water were used to feed mice for 14 days. Meanwhile, autoclaved water was fed into mice as the Control. We observed daily clinical mice parameters, and found that mice with High CPFX were nervousness and agitated from day 4 to day 18, which was not observed in other groups. And the CPFX treated mice showed anorexia from day 7 to day 18, and even longer in the High CPFX mice (until day21). Furthermore, as shown in Fig. 1b, the High CPFX mice displayed weight loss from day 18 to day 25, which was significantly lower than other groups. Meanwhile, the Low CPFX mice started to gain weight rapidly once withdraw CPFX. In addition, the CPFX treated mice did not show diarrhea during the experiment.

Mice were sacrificed at day 14, and intestinal tract tissues were harvested for TUNEL apoptosis analysis (Fig. 1c). The High CPFX mice increased apoptosis cells in duodenum than other groups, and both High and Low CPFX groups significantly increased apoptosis cells in colon. The increased apoptosis cells in High CPFX mice were correspond with decreased number of epithelial cells, goblet cells and glands in intestine epithelia in morphology. These results suggested that continuously high dosage of CPFX feeding in mice might destroy gut tract integrity by inducing apoptosis.

3.2. CPFX reduced the expression levels of tight junction proteins Ocln and ZO-1 in gut

To investigate the effects of CPFX on tight junction proteins Ocln and ZO-1, which play key roles in gut integrity [25,26], we selected different intestinal tract tissues to measure the mRNA expression of *Ocln* and *ZO-1* at day 37 after CPFX treatment. As shown in Fig. 2a, we found the High CPFX treatment exhibited clearly negative impacts on *Ocln* and *ZO-1* mRNA expression in duodenum, jejunum, ileum and colon compared with the Control group. The Low CPFX treatment reduced *Ocln* expression in intestinal tract, also decreased *ZO-1* expression in duodenum and ileum. Tight junction proteins *Ocln* and *ZO-1* were dosage dependence in different intestinal tissues after CPFX treatment, and the gut integrity did not recover at day 37 in the High CPFX group, which was confirmed by that the protein level of Ocln in the High CPFX group was still extremely low in colon relative to other groups (Fig. 2b and c). However, the Low CPFX treatment induced the mRNA level of *Ocln, ZO-1* and *muc2* which involved in mucus synthesis in colon at day 14 (Fig. 2d). Together, we speculated that the high dosage of CPFX weakened the tight junction protein Ocln and ZO-1 thus affected gut integrity. But less impact was found in the Low CPFX mice because of positive stress feedback.

3.3. CPFX impacts systemic inflammation and local inflammation in gut

We next questioned whether exposure to CPFX could alter the serum LPS levels regarding systemic inflammation, or the main immune-regulatory genes in intestinal tract (Fig. 3). The results showed that the CPFX treatment decreased LPS at day 14 compared with control mice, and there was no difference at day 37 (Fig. 3a.). We also found there were a slightly higher levels of serum IFN-γ, IL-12p70 and TNF in the High CPFX group (at day 14) than other groups (data not shown). Different from decreased LPS trends facing CPFX treatment, the MPO of duodenum increased in the High CPFX group, and both High and Low CPFX treatments induced MPO in colon at day 14 but not at day 37 (Fig. 3a.). These results demonstrated the High CPFX treatment might maintain the inflammatory cells accumulation in the intestine for a longer time, and colon was more sensitive to the changes of inflammatory cells than duodenum. Furthermore, the expression of regenerating islet-derived protein-3 gamma (reg3γ), phospholipase A2, group IIA (pla2g2α) and beta-defensin 1 (defb1) in the duodenum and colon were significantly decreased after CPFX treatments (Fig. 3b). These findings indicated that CPFX exposure diminished the antimicrobial capacity of the gut.

IL-17/IL-17R signaling are essential for regulating mucosal host defense against many invading pathogens and injured intestine repairing [27]. Commensal bacteria, especially *segmented filamentous bacteria*, are a crucial factor that drives T helper 17 (Th17) cell developments in the intestinal tract [28]. Our study showed (Fig. 3c.) that CPFX exhibited significant influences on *IL-17A* in duodenum and colon, it reduced the mRNA level of *IL-17A* even under low dosage at day 14. However, the High CPFX significantly inhibited *IL-17A* expression in duodenum but strongly promoted *IL-17A* expression in colon at day 37. There was no difference between the Low CPFX and Control regarding *IL-17A* expression at day 37. We speculated that High CPFX treatment may mainly destroy the IL-17A-secreting cells in lamina propria of duodenum because of increased apoptosis cells.

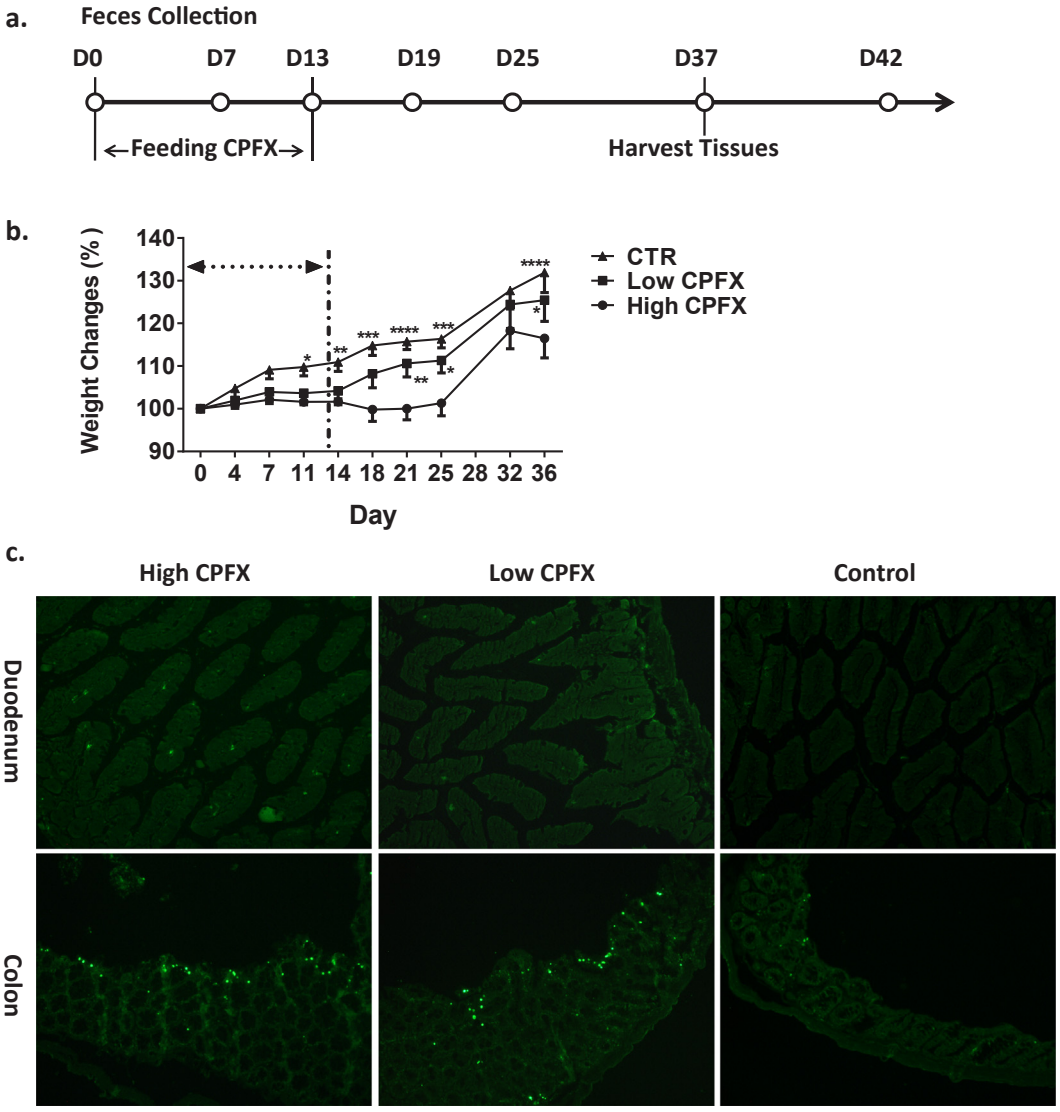

Fig. 1. The flow diagram of mouse treatment with time, the weight changes in mice with different dosage of CPFX treatments and the TUNEL apoptosis assay in duodenum and colon. (a.) The flow diagram of mouse treatment with time. CPFX treatment was from day 0 to day 13. Mouse feces were collected at day 1, day 7, and every 6 days until day 42. Intestinal tract tissues were harvest at day14 or day 37. (b.) The weight changes of mice under different dosages of CPFX treatment. CTR, mice without CPFX; Low CPFX, mice with 0.2 mg/ml CPFX; High CPFX, mice with 1 mg/ml CPFX. (c.) TUNEL apoptosis assay was performed on paraffin slides of gut tissues at day 14 in different dosages of CPFX group. Green spots represent apoptosis cells. Original magnification ×160.

However, in considering of High CPFX treatment reducing the bacterial diversity and abundance in colon, increased IL-17A level of colon was mainly devoted to host defense and repairing [29].

Once mucosal barrier function is disrupted due to toxicity of CPFX, lipopolysaccharide from luminal gram-negative bacteria activate toll-like receptor 4-signaling pathway and nucleotide-binding oligomerization domain-like receptor family, pyrin domain-containing 3 inflammasome; this leads to the release of proinflammatory cytokines IL-1β [30]. Although serum LPS levels decreased at day 14 after exposure to CPFX, the MPO levels significantly increased in the intestinal tissue (Fig. 3a). Cytokine IL-1β was intensively increased in the intestinal tract at day 37 after CPFX treatment in a dose-dependent manner, especially in duodenum (Fig. 4). Previous study illustrated that commensal-induced IL-1β production is a critical step for Th17 differentiation in the intestine [31]. Increased IL-1β boosts local antimicrobial peptides to facilitate microbiota remodeling [32]. Our results indicated that the High CPFX treatment induced IL-1β expression in different intestinal tract, these changes were probably dependent on the interconnections between gut microbiota and host immune system.

3.4. How the different dosage of CPFX impacts the gut bacteria

To check the connections between the bacterial diversity and intestinal integrity influenced by CPFX, the bacterial diversity indices in the CPFX treated mice was given (Fig. 5a.). In this study, the diversity indices in the CPFX groups show the loss of diversity compared with control group. Specifically, the High CPFX decreased the species richness (ACE and Chao indices) and had lower species diversity as explained by Shannon and Simpson indices. The similar trends were also confirmed by other alpha indices like sobs and PD_whole tree, which illustrated the alpha diversity indices were influenced strongly by different dosages of CPFX treatment. Similar research also pointed out that CPFX or levofloxacin caused the loss of intestinal bacterial diversity owing to preconditioning treatment and drug toxicity [12].

To explain the gut bacterial composition and difference in the CPFX treated and Control mice, universal primers aiming 16S rRNA gene were used to uncover the possible changes in these communities over experimental time. Fig. 5b shows the bacterial community structures exhibited big changes in response to different dosage of CPFX treatment. Families *Lactobacillaceae* and *Lachnospiraceae* exhibited high

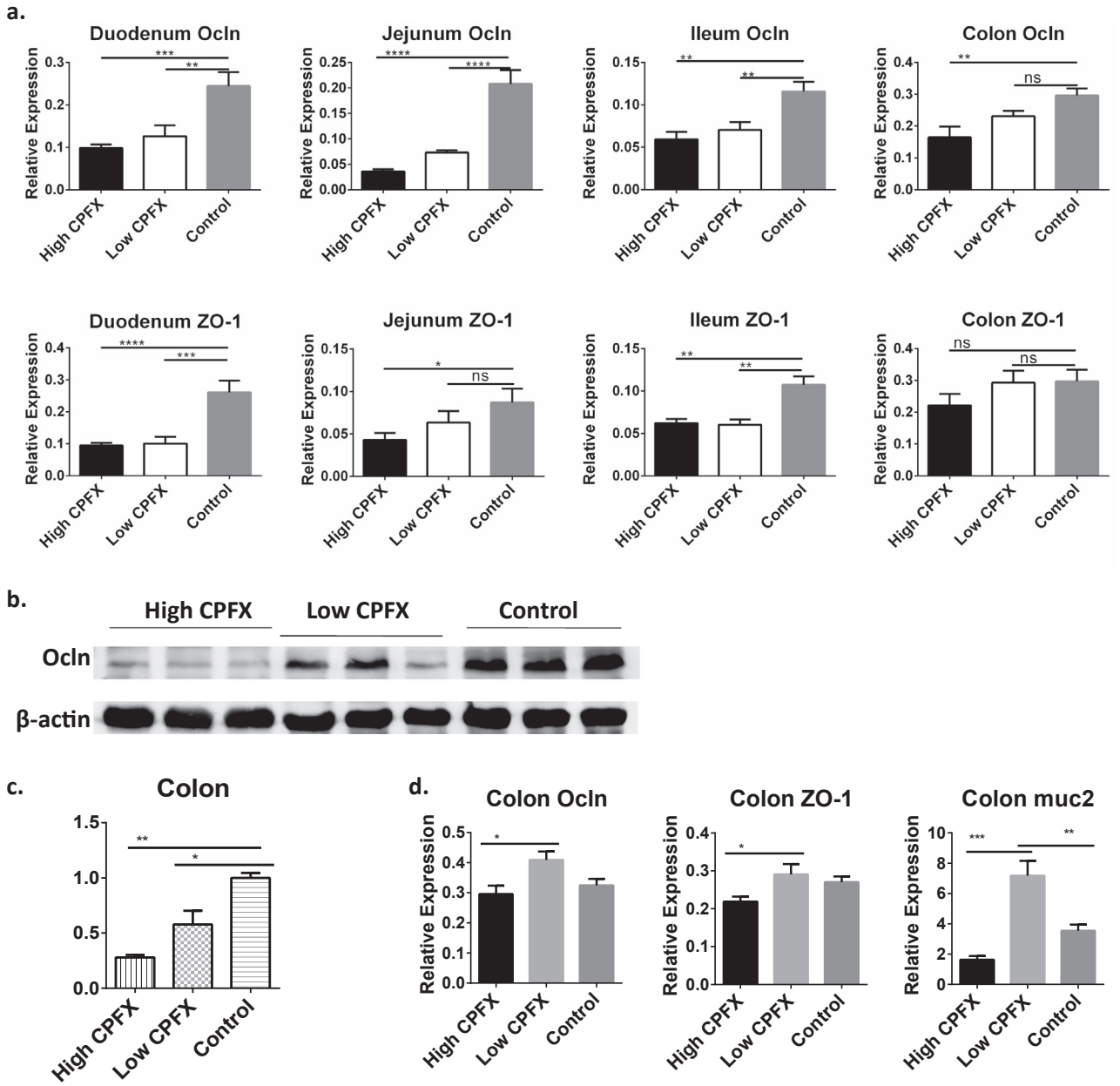

Fig. 2. The expressions of tight junction proteins on different gut tissues after CPFX treatment. (a.) Relative mRNA expression of *Ocln, ZO-1* in duodenum, jejunum, ileum and colon in High CPFX (n = 3) or Low CPFX (n = 3) or Control (n = 3) mice at day 37. Values were normalized to that of *β-actin*. Data are representative of three independent experiments. (b.) The protein expression analysis of Ocln on colon at day 37. (c.) Quantify band densitometry for Ocln on colon at day 37. (d.) Relative mRNA expression of *Ocln, ZO-1* and *muc2* in colon at day 14.

abundant levels after high dose treatment, but the relative abundant levels dropped sharply during the post period (day 49). Interestingly, the abundant level of *Verrucomicrobiaceae* populations at day 7 after high dose treatment was higher than other samples which could distinguish the High CPFX and Low CPFX. The High CPFX (day 13) and Low CPFX (day 37) had similar community structure, which probably explain even low CPFX may impact intestinal bacterial community structure. To better understand the differences in bacterial community, we analyzed the significant difference ($p < 0.05$) of bacterial population in the High CPFX and Low CPFX mice (Fig. 5c). Clearly, the CPFX treatments decreased the abundance of the intestinal bacteria compared with control mice. Observably, the significant differences of bacterial populations were detected in *Prevotellaceae*, followed by *Christensenellaceae*, *Porphyromonadaceae*, *Alcaligenaceae*, *Planococcaceae*, *Aerococcaceae*, *Peptococcaceae* and *Carnobacteriaceae*.

CPFX strongly influenced the structure of the bacterial communities in mice as illustrated by the principal co-ordinates analysis (PCA) in Fig. 5d. PCA exposed 3 different groups: a first group consisting of controls, HD_day1 and LD_day1, the second group consisting of HD_Day7, HD_Day13 and HD_Day19, and others gathered in the third group. CPFX contributed to a noticeable separation between CPFX treated mice and non-CPFX impact mice (or CPFX treated mice at day 1) in the first principal component (PC1), which explains 43.13% of the variation in the dataset.

3.5. CPFX impacts SCFAs and indole levels in mice gut

We speculated that alterations in the composition of the intestinal microbiota in mice would influence the release of metabolites after CPFX treatment. SCFAs such as butyric acid are important for intestinal

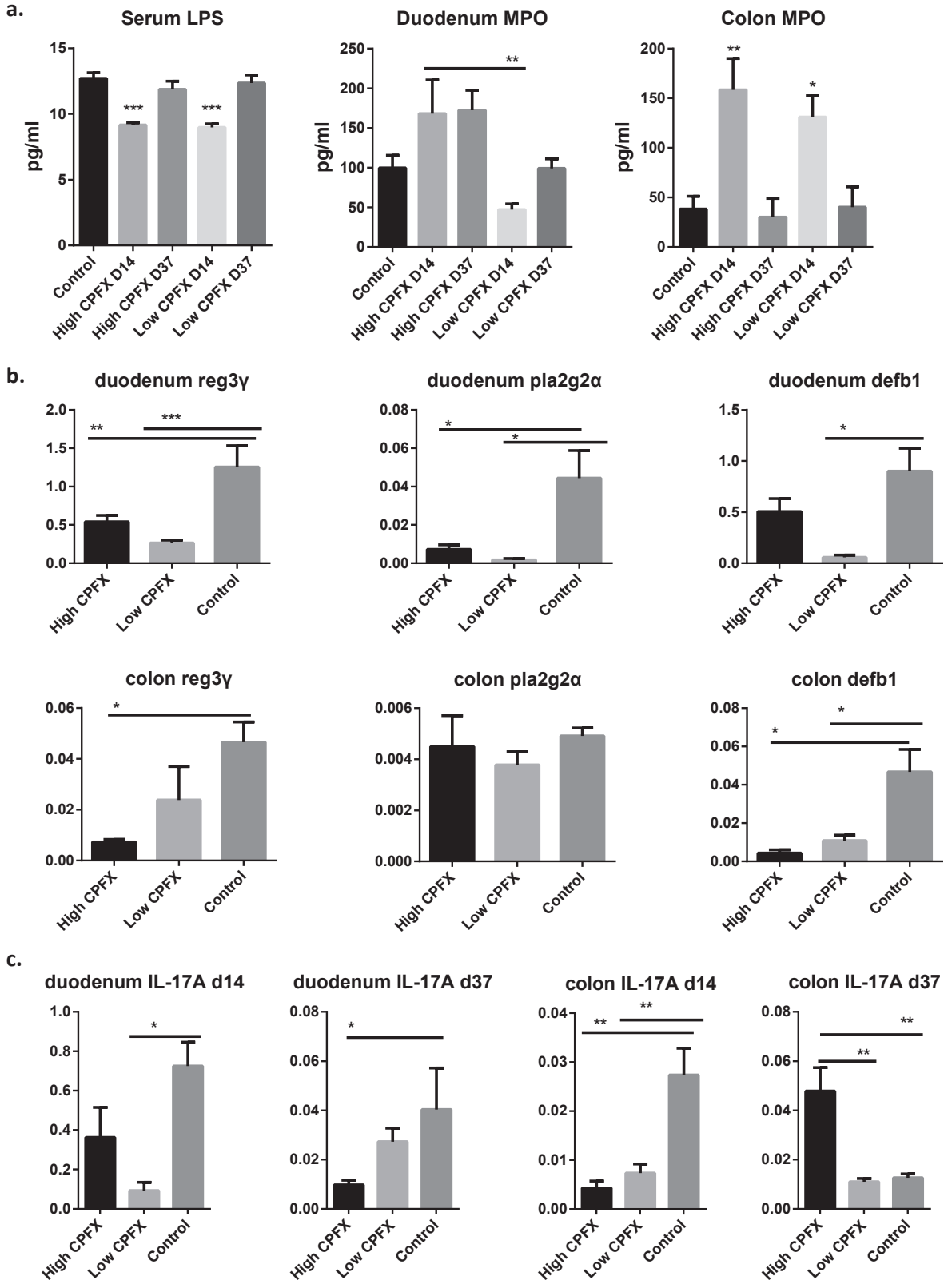

Fig. 3. The concentrations of LPS in serum and MPO in intestinal tissue, and the Mrna expressions of antimicrobial genes. (a.) The detections of serum LPS, intestinal MPO by ELISA assay. Samples were collected at day 14 and day 37. The mRNA levels of *reg3γ*, *pla2g2α*,*defb1* in duodenum and colon at day 14 (b.) and *IL-17A* in duodenum and colon at day 14 and day 37 (c.) were detected by QPCR. Values were normalized to that of *β-actin*. Data are representative of three independent experiments. Statistical significant was marked as different *P* levels.

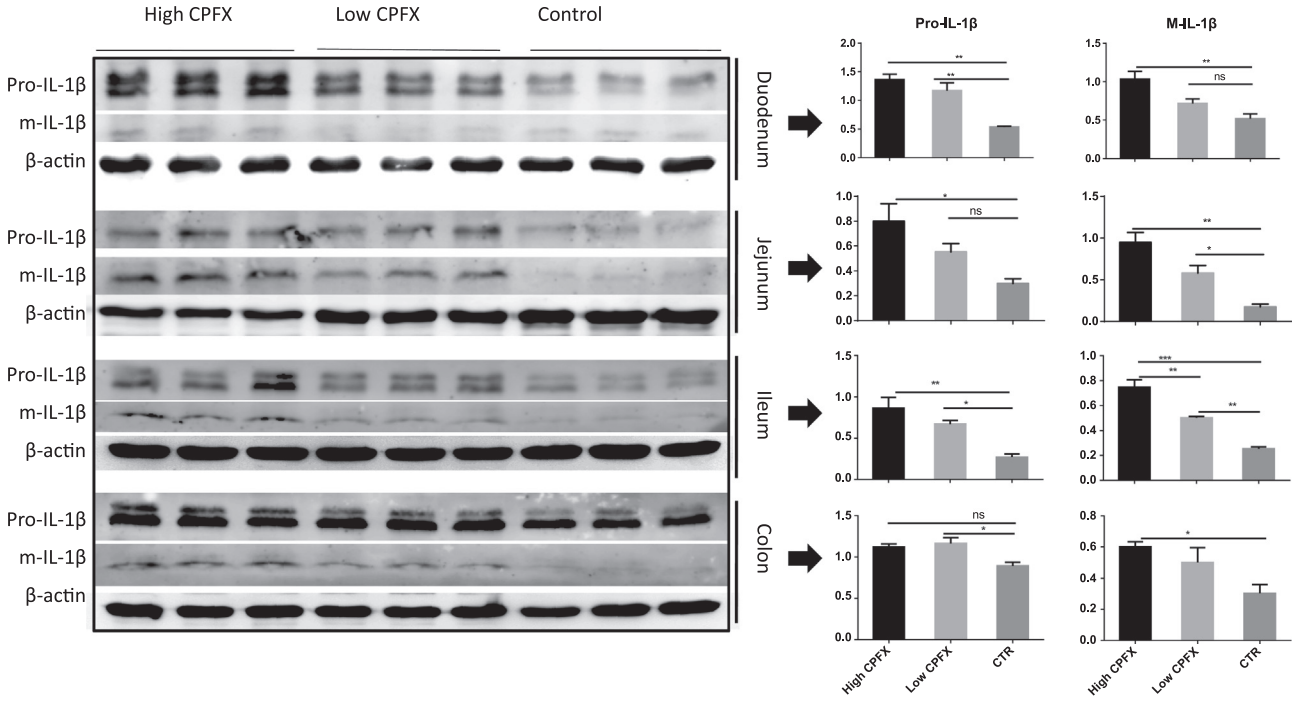

Fig. 4. Western blotting analysis of cytokine IL-1β in duodenum, jejunum, ileum and colon in High CPFX (n = 3) or Low CPFX (n = 3) or Control (n = 3) mice. Relative expressions of those proteins were shown (right). Values were normalized to that of β-actin. Data are representative of three independent experiments. Statistical significant was calculated by one-way anova and marked as different *P* levels.

microenvironment, thus maybe an important factor linking tight junctions between epithelial cells [11]. Here, we concentrated on the levels of SCFAs after CPFX treatment in mice feces as shown in Fig. 6a. Decreased acetate and propionate trends were observed after the first day of CPFX treatment, and acetate (day13) started to recover later than propionate (day 7). The butyrate concentration firstly decreased at day 1, then slightly increased at day 37 in the Low CPFX group. But the butyrate continuously decreased from day 1 to day 7, then gradually raised at day 25 in the High CPFX group. The sodium butyrate treatment did not affect the alpha diversity of intestinal microbiota during intestinal inflammation progression but altered their composition [33]. The similar trends were also found in valerate under different dosage of CPFX treatment. We speculate that CPFX has significant influences on SCFAs producing bacteria, butyrate and valerate are more sensitive to reflect the shifts of intestinal bacteria community structure than indole in mice.

Indole is vital signal molecule which has been shown to mediate intercellular signals in bacteria and enhance barrier functions of IECs [7] and even modulate immune responses in host [9]. As shown in Fig. 6a, indole exhibited sharply decline in both Low CPFX and High CPFX groups at day 7, even kept very low levels at day 13 in High CPFX, and then both gradually increased to normal level. The results demonstrated that gut bacteria especially indole producing bacteria recovered earlier in the Low CPFX group than High CPFX group. The bacterial resilient to CPFX treatment probably led to this phenomenon. Moreover, the High CPFX treatment induced low indole level for a longer time, which showed big impacts on gut bacterial diversity and metabolism homeostasis.

To explore the correlation between selected parameters and bacterial population dynamics, redundancy analysis (RDA) was analyzed in Fig. 6b. RDA presents the core bacterial population shaped the differences among samples and shows the effect of indole, butyrate and valerate on bacterial distribution in this study. The RDA plot reveals that *Lachnospiraceae*, *Verrucomicrobiaceae*, *Lactobacillaceae*, *Erysipelotrichaceae* and *Ruminococcaceae* are the main players to distinguish the High and Low CPFX treated mice over time-course. In general, indole, butyrate and valerate have similar impacts on gut bacteria in the post period of CPFX treated mice. Interestingly, non-CPFX treated mice (control) were also gathered together with LD_Day 37 and LD_Day 49. This observation may be explained by some specialized bacteria is likely rebound to syntrophs for maintaining function of butyrate and valerate generation.

3.6. Shift of bacterial linked pattern in different CPFX impacted gut

Indole, plays a core role in keeping gut homeostasis and improving intestinal barrier functions. Normally, the linked pattern between indole and gut bacteria is stable without external stimulus, but antibiotics utilization in inflammation of the intestine results in metabolic dysfunction and gut bacterial dysbiosis. In the study, the links between indole and gut bacteria were disturbed obviously under different dosage of CPFX treatment (Fig. 7). The strong correlation was only found between indole and *Bacteroidales_S247* (r = 0.61) in the Low CPFX, but the High CPFX changed the linked pattern between indole and gut bacteria which the families *Ruminococcaceae* and *Desulfovibrionaceae* strengthened the connection with indole. This phenomenon probably suggests *Ruminococcaceae* and *Desulfovibrionaceae* families are involved in restoring intestinal homeostasis. The butyrate showed significant correlation with families *Staphylococcaceae* and *Verrucomicrobiaceae* (r > 0.60) in the Low CPFX. With the CPFX dosage increment, the families *Bacteroidales_S247*, *Ruminococcaceae* and *Desulfovibrionaceae* linked closely with butyrate. It has to note that the correlation between indole and butyrate was strengthened with CPFX increment.

4. Discussion

The gut bacteria affect physiological functions through the maintenances of intestinal barrier locally to regulate metabolism including inflammation and immunity [2,34]. In this study, High CPFX treatment can significantly decrease the bacterial diversity and disturb bacterial community structure, which reduce the concentration of intermediates, such as indole and SCFAs. Further, High CPFX treatment influenced the

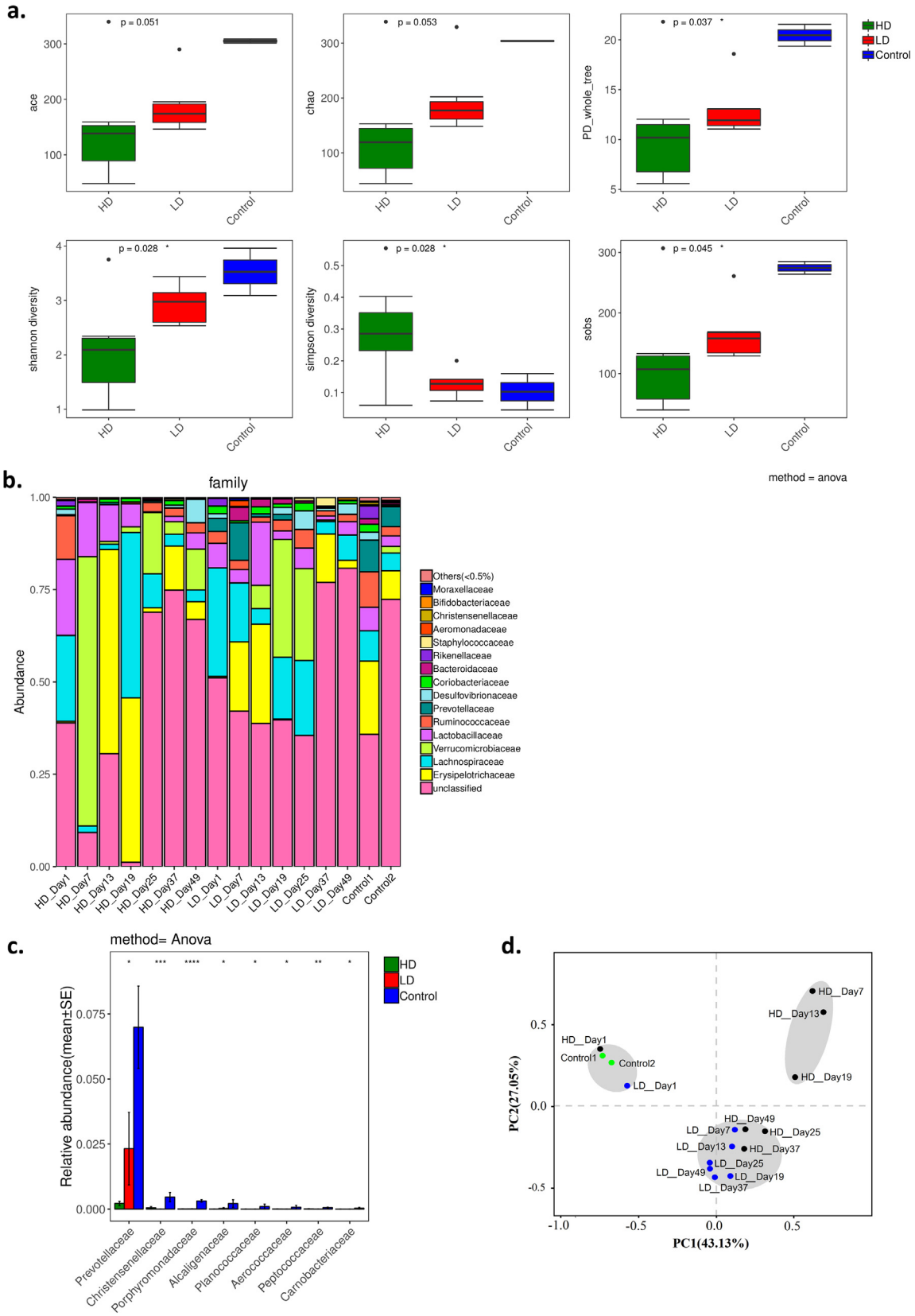

Fig. 5. Assay of alpha diversity of microbial community, microbial community composition and differential analysis on family level in different CPFX groups. (a.) ACE and Chao indices reflect species richness, Shannon and Simpson indices reflect species diversity (impacted by species richness and species evenness), and PD_whole_tree index is calculated from distance based on phylogenetic tree on OTU level, and sobs: the observed species richness. Statistical significance was calculated using the anova T test and marked as the level of the *p* values. (b.) microbial community composition ordered by cluster dendrogram based on bray-Curtis dissimilarity index in High CPFX and Low CPFX group on different days; (c.) differential analysis in High and Low CPFX group. The analysis was done on family level, only abundant level > 0.5% was included and abundant level < 0.5% was identified as unclassified. Statistical significance was calculated using the anova T test and marked as the level of the p values. (d.) PCA of microbial beta diversity indices at the operational taxonomic unit level. The High and Low CPFX feces were symbolized by different colors. The percentages in the axis labels represent the percentages of variation explained by PCA. HD, High CPFX; LD, Low CPFX.

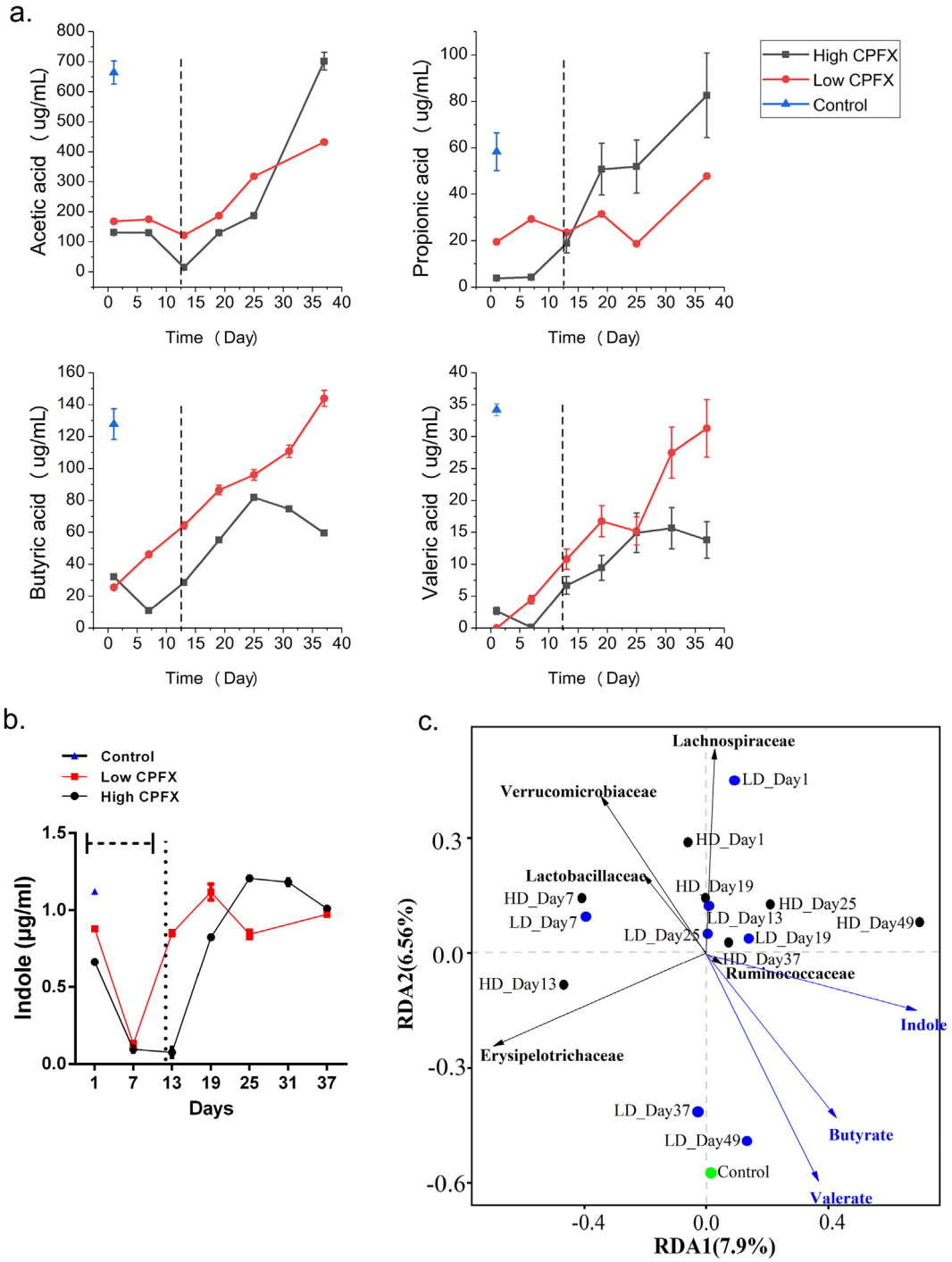

Fig. 6. The concentrations of metabolites in feces with different CPFX treatment, and the redundancy analysis. (a.) The concentration of indole and SCFAs including acetic acid, propionic acid, butyric acid and valeric acid in the feces was measured by HPLC. Horizontal dotted portion: CPFX treatment from day 0 to day 13. Mouse feces were collected at day 1, day 7, and every 6 days until day 42. (b.) RDA illustrates the separation of microbial communities on the 1st and 2nd factor planes facing different CPFX levels. Arrows indicate the correlation vectors of community differences and the selected parameters with a significant factor $p < 0.05$. Blue arrows indicate the correlation vectors of community differences and the selected parameters. Black arrows show the key intestinal bacteria influence samples distribution. The length of the arrow reflects the strength of the interaction between the selected parameters and samples' distribution. HD, High CPFX; LD, Low CPFX.

expressions of tight junction proteins and induced apoptosis cells together with inflammatory cells accumulation, which reflect the barrier damage of intestinal epithelium. On the other hand, the High CPFX treatment reduced antibacterial genes expression, increased pro-inflammatory factor IL-1β, and disturbed the concentration of IL-17A. Since antibiotic abuse in clinic has become a public health concern, great efforts are being dedicated to find effective and viable alternatives. These results suggested that the antibiotic-induced changes in gut bacteria might contribute to the inflammation responses through the alternation of metabolic status. It is necessary to treat with rational dosage of antibiotics, or narrow spectrum antibiotics for the disease prevention and treatment in future.

In general, *Firmicutes* and *Bacteroidetes* together with *Proteobacteria* are dominant in intestinal bacterial flora [35]. During the course of

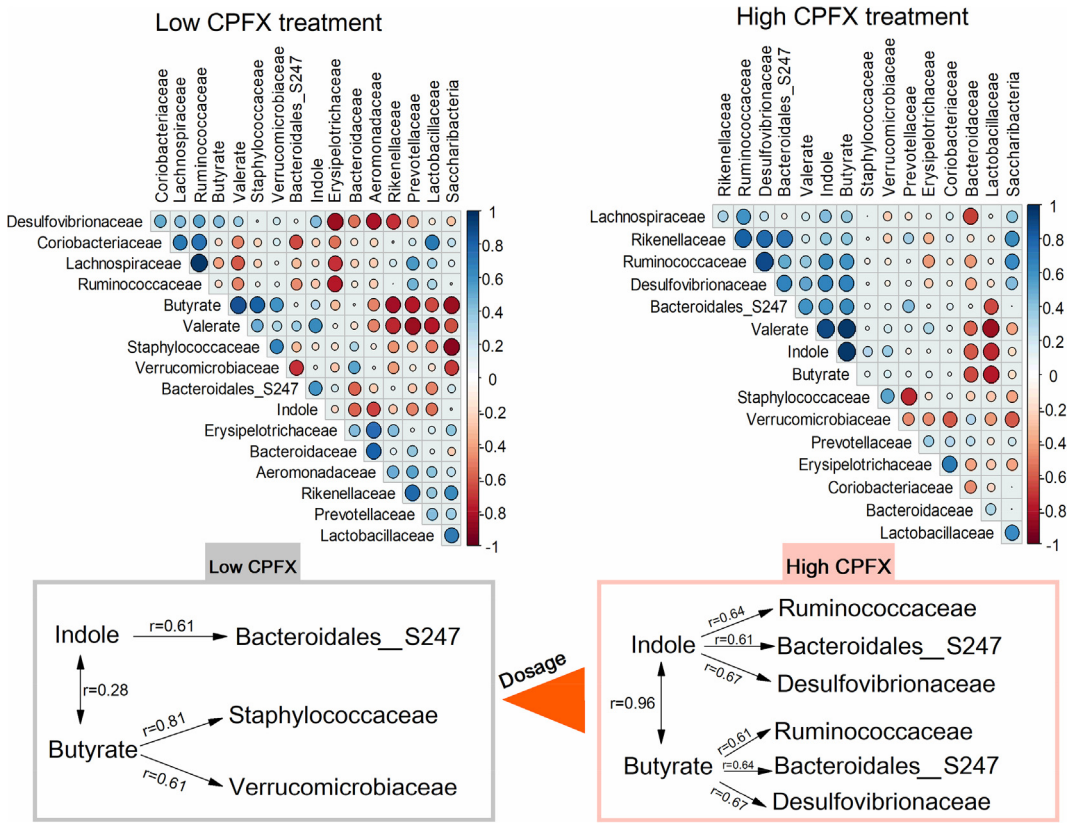

Fig. 7. Spearman's correlation analysis in the low CPFX (n = 7, $p < 0.05$) and high CPFX (n = 7, $p < 0.05$) influenced gut bacteria and selected metabolites (SCFAs and indole). The significant correlated links between butyrate/indole and gut bacteria ($r > 0.60$) were emphasized and compared in the low and high CPFX treated groups as presented in the gray and pink boxes.

antibiotics like CPFX in the study, the diversity of intestinal bacterial flora significantly decreased, which has a close link with intestinal inflammation and integrality dependent on the quantity of IECs. Recent studies manifest that low bacterial diversity in gut was associated with increased mortality caused by drug toxicity compared with a high diversity of the intestinal tract. In this study, the *Firmicutes* family *Lachnospiraceae* and *Lactobacillaceae* populations exhibited high abundant levels with High CPFX, but the relative abundant levels significantly decreased with time course facing CPFX treatment. This phenomenon may explain both *Lachnospiraceae* and *Lactobacillaceae* populations have a close relation with destroyed intestinal barrier in response to High CPFX [5,6]. Reduced IL-18 levels and expanded representation of *Prevotellaceae* existed in NLRP6$^{-/-}$ mouse colonic epithelial cells [36]. Colorectal tumor-bearing mice have low abundance of the *Prevotellaceae* family [37]. Our results showed that the CPFX treatments decreased the abundance of the intestinal bacteria compared with control mice. And the distinct bacterial populations were detected in *Prevotellaceae* which also distinguished the low and high dose treatment.

Not only bacteria themselves but also their metabolites affect host immune responses and protect against the development of inflammatory diseases [38,39]. Bacterial fermentation in the colon generates carbohydrate metabolites, including SCFAs such as acetate, butyrate and propionate. Butyrate can induce T cells by regulating molecules that improve the homing T cells to gut mucosa. In our case, the decreased trends of butyrate and tight junction proteins such as *Ocln* and *ZO-1* were detected in the intestinal tissue after CPFX treatment, which may explain the loss of butyrate consumers in gut and impaired intestine integrity. Indole, as a potential biomarker of gut microbiota health, inhibits the growth of Gram-negative bacteria [9]. In this study, *Lachnospiraceae* and *Ruminococcaceae* both affiliated to *Firmicute* families *Clostridia* class were identified as important contributors to the production of indole. And the families *Bacteroidales_S247*, *Ruminococcaceae* and *Desulfovibrionaceae*, strengthened the links with indole and butyrate regarding the CPFX dosage increment, may contribute to restore intestinal imbalances caused by intestinal inflammation and CPFX utilization.

IL-17A is a key factor in the intestinal defense process and repairing [40–42]. Published data showed that innate lymphoid cells *in situ* of the intestinal tract are preferentially involved in anti-infection immunity by secreting IL-17A. IL-17 induces IECs to secrete the antimicrobial peptide S100/β-defensin, and recruit neutrophil and macrophage through IL-8/G-CSF/MIP pathway [25]. As we found, the High CPFX treatment decreased *IL-17A* expression level in duodenum and colon at day 14 but increased *IL-17A* in colon at day 37. Therefore, we speculated that the shifts of bacterial dynamics may influence the high expression level of *IL-17A* for host defense in colon facing High CPFX treatment. Meanwhile, three important intestinal antimicrobial genes, *reg3γ, Pla2g2α and Defb1* were down-regulated in all groups exposed to CPFX in our study. These findings indicate that antibiotic exposure diminishes the antimicrobial capacity of the gut.

CRediT authorship contribution statement

Shengyun Zhu: Conceptualization, Methodology, Funding acquisition, Investigation, Writing - original draft, Writing - review & editing. **Huiqi Li:** Investigation, Formal analysis. **Jing Liang:** Data curation, Visualization. **Chaoran Lv:** Investigation, Formal analysis. **Kai Zhao:** Resources. **Mingshan Niu:** Resources. **Zhenyu Li:** Supervision, Validation. **Lingyu Zeng:** Supervision, Validation. **Kailin Xu:** Conceptualization, Funding acquisition, Supervision, Writing - review & editing.

Acknowledgments

This research were supported by National Natural Science Foundation of China (grant No. 81700179, 81930005, 81871263), the Natural Science Foundation of Jiangsu Province (grant No. BK20160226), Major Basic Research Project of the Natural Science Foundation of the Jiangsu Higher Education Institutions (grant No. 16KJA320003), the Jiangsu Science and Technology Department (grants No. BE2017638), the China Postdoctoral Science Foundation (project No. 2016M600444) and the Jiangsu Postdoctoral Research Foundation (grant No. 1601096B). All funding sources are from China. We thank Dr. Zuopeng Lv from Jiangsu Normal University for technical support and writing suggestions.

Declaration of Competing Interest

The authors declare no conflict of interest.

References

[1] V. Tremaroli, F. Backhed, Functional interactions between the gut microbiota and host metabolism, Nature 489 (7415) (2012) 242–249.
[2] Y. Shono, M.R.M. van den Brink, Gut microbiota injury in allogeneic haematopoietic stem cell transplantation, Nat. Rev. Cancer 18 (5) (2018) 283–295.
[3] H. Chu, A. Khosravi, I.P. Kusumawardhani, A.H.K. Kwon, A.C. Vasconcelos, L.D. Cunha, A.E. Mayer, Y. Shen, W.-L. Wu, A. Kambal, S.R. Targan, R.J. Xavier, P.B. Ernst, D.R. Green, D.P.B. McGovern, H.W. Virgin, S.K. Mazmanian, Gene-microbiota interactions contribute to the pathogenesis of inflammatory bowel disease, Science 352 (6289) (2016) 1116–1120.
[4] C.R. Hedin, C.J. van der Gast, A.J. Stagg, J.O. Lindsay, K. Whelan, The gut microbiota of siblings offers insights into microbial pathogenesis of inflammatory bowel disease, Gut Microbes 8 (4) (2017) 359–365.
[5] S. Huang, J. Mao, L. Zhou, X. Xiong, Y. Deng, The imbalance of gut microbiota and its correlation with plasma inflammatory cytokines in pemphigus vulgaris patients, Scand. J. Immunol. 90 (3) (2019) e12799.
[6] R. Vemuri, R. Gundamaraju, T. Shinde, A.P. Perera, W. Basheer, B. Southam, S.V. Gondalia, A.V. Karpe, D.J. Beale, S. Tristram, K.D.K. Ahuja, M. Ball, C.J. Martoni, R. Eri, Lactobacillus acidophilus DDS-1 Modulates Intestinal-Specific Microbiota, Short-Chain Fatty Acid and Immunological Profiles in Aging Mice, Nutrients 11 (6) (2019) e1297.
[7] T. Bansal, R.C. Alaniz, T.K. Wood, A. Jayaraman, The bacterial signal indole increases epithelial-cell tight-junction resistance and attenuates indicators of inflammation, PNAS 107 (1) (2010) 228–233.
[8] Y. Shimada, M. Kinoshita, K. Harada, M. Mizutani, K. Masahata, H. Kayama, K. Takeda, Commensal bacteria-dependent indole production enhances epithelial barrier function in the colon, PLoS ONE 8 (11) (2013) e80604.
[9] T. Zelante, R.G. Iannitti, C. Cunha, A. De Luca, G. Giovannini, G. Pieraccini, R. Zecchi, C. D'Angelo, C. Massi-Benedetti, F. Fallarino, A. Carvalho, P. Puccetti, L. Romani, Tryptophan catabolites from microbiota engage aryl hydrocarbon receptor and balance mucosal reactivity via interleukin-22, Immunity 39 (2) (2013) 372–385.
[10] N. Salazar, L. Valdes-Varela, S. Gonzalez, M. Gueimonde, C.G. de Los Reyes-Gavilan, Nutrition and the gut microbiome in the elderly, Gut Microbes 8 (2017) 82–97.
[11] L. Peng, Z.R. Li, R.S. Green, I.R. Holzman, J. Lin, Butyrate enhances the intestinal barrier by facilitating tight junction assembly via activation of AMP-activated protein kinase in Caco-2 cell monolayers, J. Nutr. 139 (9) (2009) 1619–1625.
[12] T. Thai, P.M. Zito, Ciprofloxacin, StatPearls, Treasure Island (FL), 2019.
[13] J.A. Karlowsky, D.C. Draghi, M.E. Jones, C. Thornsberry, I.R. Friedland, D.F. Sahm, Surveillance for antimicrobial susceptibility among clinical isolates of Pseudomonas aeruginosa and Acinetobacter baumannii from hospitalized patients in the United States, 1998 to 2001, Antimicrob. Agents Chemother. 47 (5) (2003) 1681–1688.
[14] E.J. Threlfall, J.A. Skinner, L.R. Ward, Detection of decreased in vitro susceptibility to ciprofloxacin in Salmonella enterica serotypes Typhi and Paratyphi A, J. Antimicrobial Chemotherapy 48 (5) (2001) 740–741.
[15] I. Cho, S. Yamanishi, L. Cox, B.A. Methe, J. Zavadil, K. Li, Z. Gao, D. Mahana, K. Raju, I. Teitler, H. Li, A.V. Alekseyenko, M.J. Blaser, Antibiotics in early life alter the murine colonic microbiome and adiposity, Nature 488 (7413) (2012) 621–626.
[16] D. Jankovic, J. Ganesan, M. Bscheider, N. Stickel, F.C. Weber, G. Guarda, M. Follo, D. Pfeifer, A. Tardivel, K. Ludigs, A. Bouazzaoui, K. Kerl, J.C. Fischer, T. Haas, A. Schmitt-Graff, A. Manoharan, L. Muller, J. Finke, S.F. Martin, O. Gorka, C. Peschel, J. Ruland, M. Idzko, J. Duyster, E. Holler, L.E. French, H. Poeck, E. Contassot, R. Zeiser, The Nlrp3 inflammasome regulates acute graft-versus-host disease, J. Exp. Med. 210 (10) (2013) 1899–1910.
[17] S. Zhu, P. Shi, C. Lv, H. Li, B. Pan, W. Chen, K. Zhao, Z. Yan, C. Chen, G.J. Loake, M. Niu, L. Zeng, K. Xu, Loss of NLRP3 Function Alleviates Murine Hepatic Graft-versus-Host Disease, Biol. Blood Marrow Transplant. 12 (24) (2018) 2409–2417.
[18] A. Engelbrektson, V. Kunin, K.C. Wrighton, N. Zvenigorodsky, F. Chen, H. Ochman, P. Hugenholtz, Experimental factors affecting PCR-based estimates of microbial species richness and evenness, Isme J. 4 (5) (2010) 642–647.
[19] I. Vanwonterghem, P.D. Jensen, P.G. Dennis, P. Hugenholtz, K. Rabaey, G.W. Tyson, Deterministic processes guide long-term synchronised population dynamics in replicate anaerobic digesters, Isme J. 8 (10) (2014) 2015–2028.
[20] N. Xu, G.C. Tan, H.Y. Wang, X.P. Gai, Effect of biochar additions to soil on nitrogen leaching, microbial biomass and bacterial community structure, Eur. J. Soil Biol. 74 (2016) 1–8.
[21] Q. Wang, G.M. Garrity, J.M. Tiedje, J.R. Cole, Naive Bayesian classifier for rapid assignment of rRNA sequences into the new bacterial taxonomy, Appl. Environ. Microb. 73 (16) (2007) 5261–5267.
[22] C. Quast, E. Pruesse, P. Yilmaz, J. Gerken, T. Schweer, P. Yarza, J. Peplies, F.O. Glockner, The SILVA ribosomal RNA gene database project: improved data processing and web-based tools, Nucl. Acids Res. 41 (D1) (2013) D590–D596.
[23] M. Castellari, A. Versari, U. Spinabelli, S. Galassi, A. Amati, An improved HPLC method for the analysis of organic acids, carbohydrates, and alcohols in grape musts and wines, J. Liq. Chromatogr. R T 23 (13) (2000) 2047–2056.
[24] Y. Jin, Y. Wu, Z. Zeng, C. Jin, S. Wu, Y. Wang, Z. Fu, From the Cover: exposure to oral antibiotics induces Gut Microbiota dysbiosis associated with lipid metabolism dysfunction and low-grade inflammation in mice, Toxicol. Sci.: Off. J. Soc. Toxicol. 154 (1) (2016) 140–152.
[25] A. Peck, E.D. Mellins, Precarious balance: Th17 cells in host defense, Infect. Immun. 78 (1) (2010) 32–38.
[26] G.F. Sonnenberg, L.A. Fouser, D. Artis, Border patrol: regulation of immunity, inflammation and tissue homeostasis at barrier surfaces by IL-22, Nat. Immunol. 12 (5) (2011) 383–390.
[27] S. Xu, X. Cao, Interleukin-17 and its expanding biological functions, Cell Mol. Immunol. 7 (3) (2010) 164–174.
[28] P. Kumar, L. Monin, P. Castillo, W. Elsegeiny, W. Horne, T. Eddens, A. Vikram, M. Good, A.A. Schoenborn, K. Bibby, R.C. Montelaro, D.W. Metzger, A.S. Gulati, J.K. Kolls, Intestinal interleukin-17 receptor signaling mediates reciprocal control of the Gut Microbiota and autoimmune inflammation, Immunity 44 (3) (2016) 659–671.
[29] J.A. Walker, J.L. Barlow, A.N. McKenzie, Innate lymphoid cells–how did we miss them? Nat. Rev. Immunol. 13 (2) (2013) 75–87.
[30] K. Otani, T. Tanigawa, T. Watanabe, S. Shimada, Y. Nadatani, Y. Nagami, F. Tanaka, N. Kamata, H. Yamagami, M. Shiba, K. Tominaga, Y. Fujiwara, T. Arakawa, Microbiota Plays a Key Role in Non-Steroidal Anti-Inflammatory Drug-Induced Small Intestinal Damage, Digestion 95 (1) (2017) 22–28.
[31] M.H. Shaw, N. Kamada, Y.G. Kim, G. Nunez, Microbiota-induced IL-1beta, but not IL-6, is critical for the development of steady-state TH17 cells in the intestine, J. Exp. Med. 209 (2) (2012) 251–258.
[32] X. Yao, C. Zhang, Y. Xing, G. Xue, Q. Zhang, F. Pan, G. Wu, Y. Hu, Q. Guo, A. Lu, X. Zhang, R. Zhou, Z. Tian, B. Zeng, H. Wei, W. Strober, L. Zhao, G. Meng, Remodelling of the gut microbiota by hyperactive NLRP3 induces regulatory T cells to maintain homeostasis, Nat. Commun. 8 (1) (2017) 1896.
[33] X. Zou, J. Ji, H. Qu, J. Wang, D.M. Shu, Y. Wang, T.F. Liu, Y. Li, C.L. Luo, Effects of sodium butyrate on intestinal health and gut microbiota composition during intestinal inflammation progression in broilers, Poult. Sci. 98 (10) (2019) 4449–4456.
[34] Y. Taur, R.R. Jenq, M.A. Perales, E.R. Littmann, S. Morjaria, L.L. Ling, D. No, A. Gobourne, A. Viale, P.B. Dahi, D.M. Ponce, J.N. Barker, S. Giralt, M. van den Brink, E.G. Pamer, The effects of intestinal tract bacterial diversity on mortality following allogeneic hematopoietic stem cell transplantation, Blood 124 (7) (2014) 1174–1182.
[35] P.B. Eckburg, E.M. Bik, C.N. Bernstein, E. Purdom, L. Dethlefsen, M. Sargent, S.R. Gill, K.E. Nelson, D.A. Relman, Diversity of the human intestinal microbial flora, Science 308 (5728) (2005) 1635–1638.
[36] E. Elinav, T. Strowig, A.L. Kau, J. Henao-Mejia, C.A. Thaiss, C.J. Booth, D.R. Peaper, J. Bertin, S.C. Eisenbarth, J.I. Gordon, R.A. Flavell, NLRP6 inflammasome regulates colonic microbial ecology and risk for colitis, Cell 145 (5) (2011) 745–757.
[37] J.P. Zackular, N.T. Baxter, K.D. Iverson, W.D. Sadler, J.F. Petrosino, G.Y. Chen, P.D. Schloss, The gut microbiome modulates colon tumorigenesis, mBio 4 (6) (2013) e00692–e713.
[38] L. Wen, R.E. Ley, P.Y. Volchkov, P.B. Stranges, L. Avanesyan, A.C. Stonebraker, C.Y. Hu, F.S. Wong, G.L. Szot, J.A. Bluestone, J.I. Gordon, A.V. Chervonsky, Innate immunity and intestinal microbiota in the development of Type 1 diabetes, Nature 455 (7216) (2008) 1109–U10.
[39] S.K. Mazmanian, J.L. Round, D.L. Kasper, A microbial symbiosis factor prevents intestinal inflammatory disease, Nature 453 (7195) (2008) 620–625.
[40] L.W. Kappel, G.L. Goldberg, C.G. King, D.Y. Suh, O.M. Smith, C. Ligh, A.M. Holland, J. Grubin, N.M. Mark, C. Liu, Y. Iwakura, G. Heller, M.R. van den Brink, IL-17 contributes to CD4-mediated graft-versus-host disease, Blood 113 (4) (2009) 945–952.
[41] G.F. Sonnenberg, D. Artis, Innate lymphoid cells in the initiation, regulation and resolution of inflammation, Nat. Med. 21 (7) (2015) 698–708.
[42] X.Y. Zhao, L.L. Xu, S.Y. Lu, X.J. Huang, IL-17-producing T cells contribute to acute graft-versus-host disease in patients undergoing unmanipulated blood and marrow transplantation, Eur. J. Immunol. 41 (2) (2011) 514–526.